Anomalies and Anderson localization: π-coupling of the energy bands

2009 J. Phys.: Condens. Matter 21 045503

(http://iopscience.iop.org/0953-8984/21/4/045503)

IOP PUBLISHING JOURNAL OF PHYSICS: CONDENSED MATTER

J. Phys.: Condens. Matter **21** (2009) 045503 (12pp) doi:10.1088/0953-8984/21/4/045503

Anomalies and Anderson localization: π-coupling of the energy bands

Luca Alloatti

NEST-INFM, Università di Pisa and Scuola Normale Superiore, I-56126 Pisa, Italy
and
Max-Planck Institut für Metallforschung, Heisenbergstraße 3, 70569 Stuttgart, Germany

E-mail: luca.alloatti@googlemail.com

Received 27 July 2008, in final form 27 October 2008
Published 19 December 2008
Online at stacks.iop.org/JPhysCM/21/045503

Abstract
This work shows that delocalization phenomena in single-electron quasi-one-dimensional quantum chains may occur at points different from the center of the energy spectrum ($E = 0$) and in systems lacking the symmetry $E \to -E$. It is found that the peaks appearing in the average conductance are controlled by the band structure of the periodic system underlying the disorder. The average conductance is expanded in powers of the disorder strength, allowing the conductance to be redefined as the sum of a regular and an anomalous contribution. The first non-vanishing term of the anomalous part is of the fourth order. The fourth-order term can be calculated for any number of coupled chains in terms of a matrix expression. For strictly one-dimensional systems the expansion is calculated up to the 12th order for both diagonal and real off-diagonal disorder and is compared with the numerical data. It is also found that the anomalous contribution defined here is responsible for an even–odd effect of the average conductance.

1. Introduction

It is well known that the center of the energy spectrum ($E = 0$) of the one-dimensional Anderson model (and of the many variants obtained by changing the type of disorder and the number of coupled chains) shows special features. Depending on the details of the model, it has been demonstrated that this point presents anomalies in the localization length [12, 14, 16, 22, 23, 26, 28], divergent density of states [2, 9, 13], even–odd effects [2, 18, 19], violation of single-parameter scaling (SPS) [5, 8, 21, 25, 27] and anomalously localized states (ALS) [1]. Similar features appearing at $E = 0$ have also been shown to exist in higher dimensions [6, 10, 17, 20].

Despite the numerous studies on these anomalies, some features remain to be fully understood. In particular, it is not clear what causes the point $E = 0$ to be so special. It is worth noticing that the origin of the delocalization of states of the one-dimensional hopping-disordered Anderson model has already been claimed to be due to an additional (chiral) sublattice symmetry [3, 6, 19, 18]. Additional symmetries of the Hamiltonian have also been considered as the origin of the violation of SPS at $E = 0$ [5, 8, 25].

Among the various theoretical frameworks adopted in these studies are renormalization group theory, the nonlinear σ-model, scaling theories and random matrix theory. The Møller operator [11] of conventional scattering theory has never been used so far to address the question of conductance anomalies. Although the implementation of this technique can be inconvenient as it requires inversion of large matrices, it allows us to express in a natural way the conductance in terms of a very limited number of parameters, each of which has a deep physical meaning. These are the Bloch angles, the density of states of the unperturbed system, the shape of the Bloch states and the type of disorder (see equation (14)). The energies at which the anomalies in the conductance appear must correspond to some special conditions occurring for the above-mentioned parameters.

The results described here show that, for strictly one-dimensional systems at the point $E = 0$, where the anomalies occur, the Bloch angles involved must differ by π. Analogously, for $N > 1$ coupled chains I find that at the energy $E = 0$ of the models considered in the literature there exist one or more pairs of Bloch angles such that their difference is equal to π.

I show that these are only special examples of a more general phenomenon, the 'π-coupling' of the energy bands,

described in this paper; moreover I explain the mechanism that causes the conductance to be so greatly affected by these 'π-couplings'.

2. The model

The model considered here is defined by the following Schrödinger equation (see also figure 1):

$$U_n\psi_n + T_{n-1}\psi_{n-1} + T_n^\dagger\psi_{n+1} = E\psi_n, \qquad \forall n \in \mathbb{Z}, \quad (1)$$

where U_n is the $N \times N$ matrix (N is the number of coupled chains) connecting the sites belonging to the n th column of the wire and T_n is the $N \times N$ matrix specifying the hopping amplitudes from column n to column $n+1$. The index n labels the columns along the wire (see figure 1) and ψ_n is an N-dimensional vector. The wire extends from $n = -\infty$ to ∞.

The disorder is defined by

$$U_n = U + W_n^U, \qquad T_n = T + W_n^T, \quad (2)$$

where U and T are the constant matrices defining the periodic chain system, and W_n^U and W_n^T are some randomly distributed matrices that are non-zero only for $n = 1, \ldots, \mathcal{L}$ ($\mathcal{L}$ is the length of the disordered region). The disorder matrices are given by

$$\begin{aligned}
&\left(W_n^U\right)_{i,j} \equiv w_{i,i}^U \chi_{i,i} \quad \text{for } i = j; \quad n = 1, \ldots, \mathcal{L}; \quad w_{i,i}^U \in \mathbb{R}\\
&\left(W_n^U\right)_{i,j} \equiv w_{i,j}^U \chi_{i,j} \quad \text{for } i > j; \quad n = 1, \ldots, \mathcal{L}; \quad w_{i,j}^U \in \mathbb{C}\\
&\left(W_n^U\right)_{i,j} \equiv \left(W_n^U\right)_{j,i} \quad \text{for } i < j;\\
&\left(W_n^T\right)_{i,j} \equiv w_{i,j}^T \chi_{i,j} \quad \forall\, i, j; \quad n = 1, \ldots, \mathcal{L}-1; w_{i,j}^T \in \mathbb{C}
\end{aligned} \quad (3)$$

where every χ represents a random number in $[-1/2, 1/2]$. All the χs appearing in the previous definition are *independent* stochastic variables. Therefore all the random numbers added to the Hamiltonian are in general different (compatible with the constraint $H = H^\dagger$). Notice that the disorder on the self-energies (diagonal disorder) is represented only by the *diagonal* of the W_n^U matrices while all the other terms represent the hopping disorder (off-diagonal disorder).

For later uses (see section 4), the 'global' rescaling of the disorder is defined by rescaling both matrices $w_{i,j}^T$ and $w_{i,j}^U$ according to

$$w_{i,j}^{T(U)} \to w_G w_{i,j}^{T(U)}, \qquad w_G \in \mathbb{R}^+. \quad (4)$$

3. Conductance in terms of the Møller operator and consequences

It is well known that the *free* Hamiltonian H_0 of the system can be diagonalized by means of Bloch states. These states can be written in the following form:

$$\begin{aligned}
&\phi_n(\theta_B, \nu) \equiv Z_{\theta_B}^\nu \, e^{in\theta_B}, \qquad \theta_B \in [-\pi, \pi],\\
&\nu = 1, \ldots, N, \quad n \in \mathbb{Z};
\end{aligned} \quad (5)$$

where θ_B is the Bloch angle of the state, ν is the 'channel' index and $Z_{\theta_B}^\nu$ is defined as the νth column of an $N \times N$ unitary matrix Z_{θ_B} diagonalizing the following Hermitian matrix:

$$Q = T\, e^{-i\theta_B} + U + T^\dagger e^{i\theta_B}. \quad (6)$$

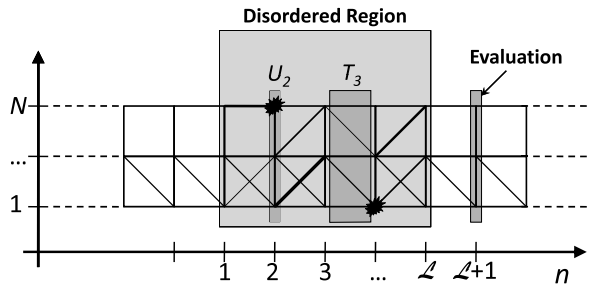

Figure 1. Scheme of the multichain system with $N = 3$. The diagonal disorder is indicated by means of spiky shapes and the off-diagonal disorder by means of lines of different thicknesses. The column indicated as 'evaluation' is used in equation (10) to evaluate the transmission amplitudes.

The cases where, on the left of the disordered region, there is only one Bloch state with positive group velocity (defined by $v_g(\theta, \nu) \equiv \frac{1}{\hbar}\frac{\partial E(\theta,\nu)}{\partial\theta}$) and on the right there is no state with negative group velocity, are used to define the conductance. These cases are described by

$$\psi_n^{(\eta)} = \begin{cases} \phi_n\left(\theta_\eta^+(E), \eta\right) \\ \quad + \displaystyle\sum_\nu A_{\eta\to\nu}^R \phi_n\left(\theta_\nu^-(E), \nu\right) & \text{for } n < 1 \\ \displaystyle\sum_\nu A_{\eta\to\nu}^T \phi_n\left(\theta_\nu^+(E), \nu\right) & \text{for } n > \mathcal{L}, \end{cases} \quad (7)$$

where the amplitudes $A^{T(R)}$ are determined by requiring $\psi_n^{(\eta)}$ to be an eigenvector of the complete Hamiltonian $H = H_0 + W$.

The conductance at the energy E is then expressed only in terms of the transmission amplitudes:

$$g(E) = 2e^2 \sum_{\eta,\nu} D(E, \eta)|A_{\eta\to\nu}^T|^2 v_g(E, \nu), \quad (8)$$

where $D(E, \eta) = \frac{1}{2\pi}|\frac{\partial E(\theta,\eta)}{\partial\theta}|^{-1}$ is the density of states per unit length in the channel η at energy E.

The state $\psi^{(\eta)}$ in equation (7), and hence the transmission amplitudes A^T, can be obtained directly by applying the Møller operator Ω^+ (defined abstractly by $\Omega^+ \equiv \lim_{t\to\infty} e^{-iHt} e^{iH_0 t}$, see section 3.5 or see [11]) to the Bloch state $\phi(\theta_\eta^+, \eta)$:

$$\psi^{(\eta)} \equiv \Omega^+ \phi(\theta_\eta^+, \eta). \quad (9)$$

Starting from equation (9), it can be seen that, if the matrix Z_{θ_B} is constant in θ_B (see section 3.3), the transmission amplitude is given by (see an example of its application in section 3.4)

$$A^T(\eta \to \nu) = \left\langle \begin{pmatrix} 0 \\ 0 \\ \vdots \\ \hat{e}_\nu \end{pmatrix} \left| \frac{1}{1 - \mathbb{F}\widetilde{\mathbb{G}}\widetilde{\mathbb{W}}} \right| \begin{pmatrix} \hat{e}_\eta\, e^{i\theta_\eta^+} \\ \hat{e}_\eta\, e^{i2\theta_\eta^+} \\ \vdots \\ \hat{e}_\eta\, e^{i(\mathcal{L}+1)\theta_\eta^+} \end{pmatrix} \right\rangle. \quad (10)$$

Table 1. Eigenvalues of the free Green's function and phases; $\lambda_\eta^U(T)$ are the eigenvalues of $U(T)$ which exist because of the hypothesis Z_{θ_B} = constant. In this case the bands are given by $E(\theta_B, \eta) = \lambda_\eta^U + 2\lambda_\eta^T \cos(\theta_B)$.

	$\widetilde{G}_{\eta,\eta}$	$(F_n)^{\pm}_{\eta,\eta}$
$2 < \frac{\lambda_\eta^U - E}{\lambda_\eta^T}$	$-\frac{1}{\lambda_\eta^U\sqrt{4-\left(\frac{\lambda_\eta^U-E}{\lambda_\eta^T}\right)^2}}$	$\left[\frac{-\frac{\lambda_\eta^U-E}{\lambda_\eta^T}-\sqrt{\left(\frac{\lambda_\eta^U-E}{\lambda_\eta^T}\right)^2-4}}{2}\right]^{\lvert n\rvert}$
$-2 < \frac{\lambda_\eta^U - E}{\lambda_\eta^T} < 2$	$-\mathrm{i}\frac{1}{\lvert\lambda_\eta^U\rvert\sqrt{4-\left(\frac{\lambda_\eta^U-E}{\lambda_\eta^T}\right)^2}}$	$\left[\frac{-\frac{\lambda_\eta^U-E}{\lambda_\eta^T}+\mathrm{i}\sqrt{\left(\frac{\lambda_\eta^U-E}{\lambda_\eta^T}\right)^2-4}}{2}\right]^{\lvert n\rvert}$ for $\lambda_{\eta,\eta}^T < 0$
		$\left[\frac{-\frac{\lambda_\eta^U-E}{\lambda_\eta^T}-\mathrm{i}\sqrt{\left(\frac{\lambda_\eta^U-E}{\lambda_\eta^T}\right)^2-4}}{2}\right]^{\lvert n\rvert}$ for $\lambda_{\eta,\eta}^T > 0$
$\frac{\lambda_\eta^U - E}{\lambda_\eta^T} < -2$	$\frac{1}{\lambda_\eta^U\sqrt{4-\left(\frac{\lambda_\eta^U-E}{\lambda_\eta^T}\right)^2}}$	$\left[\frac{-\frac{\lambda_\eta^U-E}{\lambda_\eta^T}+\sqrt{\left(\frac{\lambda_\eta^U-E}{\lambda_\eta^T}\right)^2-4}}{2}\right]^{\lvert n\rvert}$

The meaning of the symbols entering in equation (10) is specified below:

- $\hat{e}_\nu$ is the vector of dimension N having one at the νth position and zero elsewhere. The different rows of the bracketed states correspond to the values $n = 1, \ldots, \mathcal{L}+1$.
- $\widetilde{\mathbb{W}}$ is given by

$$\widetilde{\mathbb{W}} = \mathbb{Z}^\dagger (DWD)\mathbb{Z},$$

  where D is the projector (with finite image size, see section 3.5) on the subspace $n = 1, \ldots, \mathcal{L}+1$ containing the disorder and $\mathbb{Z}$ is the $(\mathcal{L}+1)N \times (\mathcal{L}+1)N$ *block-diagonal* matrix with blocks equal to Z.
- $\widetilde{\mathbb{G}}$ is the *block-diagonal* matrix with blocks equal to $\widetilde{G} \equiv Z^\dagger G Z$ (G is the *free* Green's function projected onto the left and onto the right of the same column).
- The matrix $\mathbb{F}$ is defined by

$$\mathbb{F} = \begin{pmatrix} \mathbb{I} & F_1^- & \cdots & F_{\mathcal{L}}^- \\ F_1^+ & \mathbb{I} & \cdots & F_{\mathcal{L}-1}^- \\ \vdots & \vdots & \ddots & \vdots \\ F_{\mathcal{L}}^+ & F_{\mathcal{L}-1}^+ & \cdots & \mathbb{I} \end{pmatrix}, \tag{11}$$

  where $\mathbb{I}$ is the $N \times N$ unit matrix and $F_n^\pm$ are defined below.
- The matrices $\widetilde{G}$ and $F_n^\pm$ are $N \times N$ *diagonal* matrices given by

$$\widetilde{G} = \begin{pmatrix} \widetilde{G}_{1,1} & 0 & \cdots & 0 \\ 0 & \widetilde{G}_{2,2} & \cdots & 0 \\ \vdots & \vdots & \ddots & 0 \\ 0 & 0 & 0 & \widetilde{G}_{N,N} \end{pmatrix};$$
$$F_n^\pm = \begin{pmatrix} (F_n)^\pm_{1,1} & 0 & \cdots & 0 \\ 0 & (F_n)^\pm_{2,2} & \cdots & 0 \\ \vdots & \vdots & \ddots & 0 \\ 0 & 0 & 0 & (F_n)^\pm_{N,N} \end{pmatrix}, \tag{12}$$

  where the ηth diagonal element corresponds to the ηth band as given in table 1.

In the case that $-2 < \frac{\lambda_\eta^U - E}{\lambda_\eta^T} < 2$ (i.e. in the case that the ηth band possesses states with energy E), $\widetilde{G}_{\eta,\eta}$ and $(F_n)^\pm_{\eta,\eta}$ can be expressed only in terms of the band derivatives and of the Bloch angles:

$$\boxed{\begin{aligned} &\widetilde{G}_{\eta,\eta} = -\mathrm{i}2\pi D(E,\eta) = -\mathrm{i}\left|\tfrac{\partial E(\theta,\nu)}{\partial\theta}\right|^{-1}, \\ &(F_n)^\pm_{\eta,\eta} = \mathrm{e}^{\pm \mathrm{i}\theta_\eta^\pm n}, \end{aligned}} \tag{13}$$

where $\theta_\eta^{+(-)}$ are the Bloch angles at which the ηth band has energy E and positive (+) or negative (−) group velocity.

3.1. Consequences for the conductance

Equations (10) and (13) immediately imply that, under the following assumptions:

- the Bloch-states matrix $Z \equiv Z_{\theta_B}$ is constant (see section 3.3),
- at the energy E all the bands are present,

the average conductance $\langle g(E)\rangle$ of a system can be expressed as a function of the following quantities only:

- the $2N$ Bloch angles $\theta_\nu^\pm(E)$,
- the $2N$ derivatives $\frac{\partial E(\theta,\eta)}{\partial\theta}|_{\theta_\eta^\pm(E)}$,
- the constant matrix Z,
- the type of disorder (i.e. $\mathcal{L}$ and the coefficients in equation (3)).

In other words, one can write

$$\boxed{\langle g\rangle = \langle g\rangle\left(\left\{\theta_\nu^\pm\right\}, \left\{\widetilde{G}_{\eta,\eta}\right\}, Z, \mathcal{L}, \left\{w_{i,j}^{T(U)}\right\}\right).} \tag{14}$$

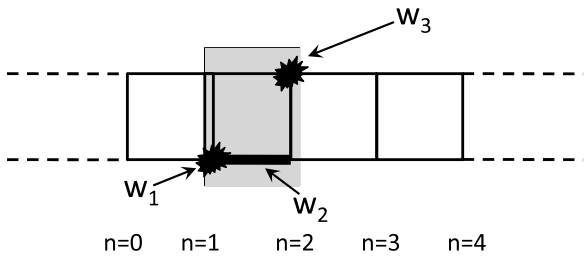

Figure 2. Sketch of the example considered in this section. It consists of a disordered region of length $\mathcal{L} = 2$ where two sites have diagonal disorder (spiky shapes) and one hopping has off-diagonal disorder (thicker line).

3.2. Important corollaries

If a system satisfies the hypothesis given in section 3.1 and also exhibits a peak in the average conductance $g(E)$ for some special energies, these particular energies must be associated with a special condition occurring on the Bloch angles $\theta_\nu^\pm(E)$ and/or on the derivatives $\frac{\partial E(\theta,\nu)}{\partial\theta}|_{\theta_\nu^\pm(E)}$. This is because the other quantities in equation (14) remain constant when the energy is varied.

For a single chain, it can immediately be seen that the derivatives $\frac{\partial E(\theta,\nu)}{\partial\theta}|_{\theta_\nu^\pm(E)}$ do not show any special behavior when the energy is varied around zero (these derivatives have neither special values nor variations of the symmetry). It can hence be concluded that the angles involved are at the origin of the peak observed. Moreover, the observation that, at the center of the energy spectrum ($E = 0$) of any one-dimensional system the Bloch angles are such that $\theta^+ - \theta^- = \pm\pi$ (the band structure is always a single cosine), implies that this condition is responsible for the appearance of the peaks.

For a larger number of coupled chains it is, however, not possible to show using simple arguments that the derivatives $\frac{\partial E(\theta,\nu)}{\partial\theta}$ do not play a role in the appearance of the peaks, since symmetry properties of these values (like $\frac{\partial E(\theta,\nu)}{\partial\theta} = \frac{\partial E(\theta,\eta)}{\partial\theta}$ for $\nu \neq \eta$) might appear as the energy is varied. However, by performing a perturbative expansion of the average conductance, it is shown in this paper that the appearance of the peaks is due uniquely to the fact that a class of diagrams sum up coherently whenever there exists a pair of bands (ν, η) and an integer q such that $\theta_\nu^+ - \theta_\eta^- = q\pi$. For convenience, the occurrence of such a condition will be called 'π-coupling of the energy bands'.

3.3. The assumption $Z_{\theta_B} = constant$

The assumption that Z_{θ_B} (defined by equation (6)) is independent of θ_B is equivalent to saying that the shape of the Bloch states remains the same along each band. This assumption is motivated by the fact that most of the models considered in the previous works satisfy the same condition. Moreover the whole mathematical formalism is greatly simplified without hiding the mechanism responsible for the resonances. Stating that Z_{θ_B} is constant is equivalent to saying that the matrices U and T are both diagonalizable and have a common basis of eigenvectors. Otherwise, a *sufficient* condition for Z_{θ_B} to be constant is that $T^\dagger = T$ and the commutator $[T, U]$ vanishes (e.g. when U is a multiple of the identity, as is usually assumed, or when there is a single chain).

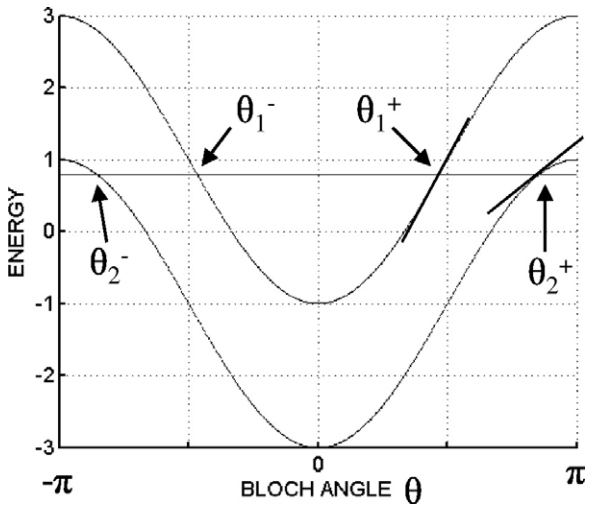

Figure 3. Band structure of the perfect two-chain system. In this figure the energy $E = 0.8$ is chosen as an example to define the Bloch angles $\theta_{1(2)}^\pm$ and the derivatives involved.

3.4. Example of use of the transmission amplitude equation

As an example one can consider the two coupled chains of figure 2, where w_1 and w_2 are diagonal disorders and w_2 is a hopping disorder. Let us suppose that the hoppings of the unperturbed system are equal to -1 and that the on-site energies are equal to zero. The Hamiltonian $H = H_0 + W$ of the complete system is then given by

$$\left(\begin{array}{c|ccc|c} \ddots & \vdots & \vdots & \vdots & \\ \hline \cdots & U_1 & T_1^\dagger & 0 & \cdots \\ \cdots & T_1 & U_2 & T_2^\dagger & \cdots \\ \cdots & 0 & T_2 & U_3 & \cdots \\ \hline & \vdots & \vdots & \vdots & \ddots \end{array}\right) =$$

$$\left(\begin{array}{c|cc|cc|cc|c} \ddots & \vdots & \vdots & \vdots & \vdots & \vdots & \vdots & \\ \hline \cdots & w_1 & -1 & -1+w_2^* & 0 & 0 & 0 & \cdots \\ \cdots & -1 & 0 & 0 & -1 & 0 & 0 & \cdots \\ \hline \cdots & -1+w_2 & 0 & 0 & -1 & -1 & 0 & \cdots \\ \cdots & 0 & -1 & -1 & w_3 & 0 & -1 & \cdots \\ \hline \cdots & 0 & 0 & -1 & 0 & 0 & -1 & \cdots \\ \cdots & 0 & 0 & 0 & -1 & -1 & 0 & \cdots \\ \hline & \vdots & \vdots & \vdots & \vdots & \vdots & \vdots & \ddots \end{array}\right). \tag{15}$$

The unperturbed system has two bands, which are shown in figure 3. The Bloch states are given by

$$\begin{aligned} \phi_n(\theta_1, \nu = 1) &= \frac{1}{\sqrt{2}}\begin{pmatrix} 1 \\ -1 \end{pmatrix} e^{in\theta_1}, \\ \phi_n(\theta_2, \nu = 2) &= \frac{1}{\sqrt{2}}\begin{pmatrix} 1 \\ 1 \end{pmatrix} e^{in\theta_2} \end{aligned} \tag{16}$$

therefore the matrix Z is given by $Z = \frac{1}{\sqrt{2}}\left(\begin{smallmatrix} 1 & 1 \\ -1 & 1 \end{smallmatrix}\right)$.

The matrices $\mathbb{F}$, $\widetilde{\mathbb{G}}$ and $\widetilde{\mathbb{W}}$ appearing in equation (10) are given by

$$\mathbb{F} = \left(\begin{array}{cc|cc|cc} 1 & 0 & e^{-i\theta_1^-} & 0 & e^{-i2\theta_1^-} & 0 \\ 0 & 1 & 0 & e^{-i\theta_2^-} & 0 & e^{-i2\theta_2^-} \\ \hline e^{i\theta_1^+} & 0 & 1 & 0 & e^{-i\theta_1^-} & 0 \\ 0 & e^{i\theta_2^+} & 0 & 1 & 0 & e^{-i\theta_2^-} \\ \hline e^{i2\theta_1^+} & 0 & e^{i\theta_1^+} & 0 & 1 & 0 \\ 0 & e^{i2\theta_2^+} & 0 & e^{i\theta_2^+} & 0 & 1 \end{array}\right) \tag{17}$$

$$\widetilde{\mathbb{G}} = \left(\begin{array}{cc|cc|cc} \frac{-i}{\left|\frac{\partial E(\theta,1)}{\partial\theta}\right|} & 0 & 0 & 0 & 0 & 0 \\ 0 & \frac{-i}{\left|\frac{\partial E(\theta,2)}{\partial\theta}\right|} & 0 & 0 & 0 & 0 \\ \hline 0 & 0 & \frac{-i}{\left|\frac{\partial E(\theta,1)}{\partial\theta}\right|} & 0 & 0 & 0 \\ 0 & 0 & 0 & \frac{-i}{\left|\frac{\partial E(\theta,2)}{\partial\theta}\right|} & 0 & 0 \\ \hline 0 & 0 & 0 & 0 & \frac{-i}{\left|\frac{\partial E(\theta,1)}{\partial\theta}\right|} & 0 \\ 0 & 0 & 0 & 0 & 0 & \frac{-i}{\left|\frac{\partial E(\theta,2)}{\partial\theta}\right|} \end{array}\right) \tag{18}$$

$$\widetilde{\mathbb{W}} = \left(\begin{array}{cc|cc|cc} w_1 & -w_1 & -w_2^* & w_2^* & 0 & 0 \\ -w_1 & w_1 & -w_2^* & w_2^* & 0 & 0 \\ \hline -w_2 & -w_2 & w_3 & w_3 & 0 & 0 \\ w_2 & w_2 & w_3 & w_3 & 0 & 0 \\ \hline 0 & 0 & 0 & 0 & 0 & 0 \\ 0 & 0 & 0 & 0 & 0 & 0 \end{array}\right) \tag{19}$$

where $\theta^{\pm}_{1(2)}$ and the derivatives $\frac{\partial E(\theta,1(2))}{\partial\theta}$ are also shown in figure 3. Using the matrices just defined, the transmission amplitude from the band $\eta = 1$ to the band $\nu = 2$ for example becomes

$$A^{\mathrm{T}}(1\to 2) = \left(\begin{array}{cc|cc|cc} 0 & 0 & 0 & 0 & 0 & 1 \end{array}\right)\left[\mathbb{I} - \mathbb{F}\widetilde{\mathbb{G}}\widetilde{\mathbb{W}}\right]^{-1} \times \left(\begin{array}{c} e^{i\theta_1^+} \\ 0 \\ \hline e^{i2\theta_1^+} \\ 0 \\ \hline e^{i3\theta_1^+} \\ 0 \end{array}\right). \tag{20}$$

3.5. Derivation of the transmission amplitude equation

The abstract definition of the Møller operator Ω^+ is given by the following limit (see, e.g., [11]):

$$\Omega^+ \equiv \lim_{t\to\infty} e^{-iHt}\, e^{iH_0 t}. \tag{21}$$

This means that Ω^+ makes first a *free* evolution from the present to a remote time in the past (which has the effect of a *translation* if the wavefunction has a well-defined group velocity), followed by a *complete* evolution from that past to the present, which has the effect of 'throwing' the wavepacket on the scatterers. This intuitively justifies the validity of

$$\Omega^+\phi_n\left(\eta, \theta_\eta^+(E)\right) = \begin{cases} \phi_n\left(\eta, \theta_\eta^+(E)\right) + \sum_\nu A^R_{\eta\to\nu}\phi_n\left(\theta_\nu^-(E), \nu\right), & n < 1 \\ \sum_\nu A^{\mathrm{T}}_{\eta\to\nu}\phi_n\left(\theta_\nu^+(E), \nu\right) & \text{for } n > \mathcal{L}, \end{cases} \tag{22}$$

as already seen in equation (7).

When the Møller operator is applied on an eigenstate ϕ of the free Hamiltonian, it can be written in a particularly simple form. It can be shown that (see [11])

$$\Omega^+\phi(\theta_\eta^+, \eta) = \left(1 + \frac{1}{E - H + i\epsilon}W\right)\phi(\theta_\eta^+, \eta) \tag{23}$$

$$= \left(\frac{1}{1 - G(E)W}\right)\phi(\theta_\eta^+, \eta) \tag{24}$$

where

- $E \equiv E(\theta_\eta^+, \eta)$,
- $W \equiv H - H_0$ is the matrix of disorder,
- $G(E)$ is the retarded Green's function of the *free* system; $G(E) \equiv 1/(E - H_0 + i\epsilon)$,
- Dyson's equation was used to derive (24) from equation (23).

In the last equation, all the matrices are actually $\infty \times \infty$. In order to obtain an equation which can be implemented numerically, the problem has to be reduced to a *finite*-dimensional one. This can be done because the disorder matrix W is non-zero only in the *finite* submatrix corresponding to the sites in $n = 1, \ldots, \mathcal{L}$; the derivation is shown below.

From equations (7) and (8) it follows that, in order to calculate the transmission amplitudes $\{A^{\mathrm{T}}_{\eta\to\nu}\}$, it is enough to know the outgoing wavefunction $\psi_n^{(\eta)}$ only in a *finite* region on the right side of the disorder; this is the 'evaluation' column indicated in figure 1. It is hence enough to evaluate the left-projected matrix $P_B\Omega^+$, where P_B is the projector over some finite region B larger than the disordered region. The fact that the Møller operator, as given by equation (23), has the disorder matrix W on its right allows the Møller operator to be projected also on the right.

Before continuing, it is necessary to define two auxiliary operators. These operators differ from the standard projectors because of the dimensions of their image space and domain space. I define the operators D_B and $\overline{D_B}$ in the following way (in this definition B denotes a generic region of the wire, i.e. a subspace of the Hilbert space $\mathbb{C}^\infty$):

if M is a generic $\infty \times \infty$ matrix, then

- MD_B is the matrix of size $\infty \times b$ (b is the dimension of the B subspace) defined by dropping all the *columns* which do not correspond to the subspace B,
- D_BM is the matrix of size $b \times \infty$ defined by dropping all the *raws* which do not correspond to the subspace B.

The operator $\overline{D_B}$ is defined so as to perform the inverse operation of D_B. In particular, if $M^{(B)}$ is an $\infty \times \infty$ matrix such that its image is in B and such that the complement to B is in its kernel (i.e. $P_BM^{(B)}P_B = M^{(B)}$), then $\overline{D_B}D_BM^{(B)} = M^{(B)}\overline{D_B}D_B = M^{(B)}$. In practice $\overline{D_B}$ restores the null columns or rows which D_B eliminates.

The reason for introducing the operators D_B and $\overline{D_B}$ is also to avoid the confusion due to the fact that, if Ω is an invertible matrix (and the region B is not the hole wire), then $P_B\Omega P_B$ is not invertible but $D_B\Omega D_B$ is invertible.

It is possible now to continue the derivation starting from equation (24):

$$\begin{aligned}
P_B\Omega^+ &= P_B\left(\frac{1}{1-GW}\right)\\
&= P_B\,(1+GW+GWGW+GWGWGW+\cdots)\\
&= P_B\,(1+G(P_BWP_B)+G(P_BWP_B)G(P_BWP_B)+\cdots)\\
&= P_B(1+G(P_BWP_B)+G(P_BWP_B)G(P_BWP_B)+\cdots)P_B\\
&= \overline{D_B}D_B(1+G(P_BWP_B)\\
&\quad +G(P_BWP_B)G(P_BWP_B)+\cdots)D_B\overline{D_B}\\
&= \overline{D_B}\,(1_{BB}+G_{BB}W_{BB}+G_{BB}W_{BB}G_{BB}W_{BB}+\cdots)\,\overline{D_B}\\
&= \overline{D_B}\left(\frac{1_{BB}}{1_{BB}-G_{BB}W_{BB}}\right)\overline{D_B} \qquad (25)
\end{aligned}$$

where the subscript $_{BB}$ denotes the application of the operator D_B both on the left and on the right. The important feature of equation (25) is that the expression between parentheses is a *finite* matrix which can be inverted numerically (specifically I used the LAPACK Fortran libraries, see http://www.netlib.org/lapack/).

The final amplitude equation in (10) follows by means of

$$\begin{aligned}
\mathbb{Z}^\dagger\Omega_{+,BB}\mathbb{Z} &= \mathbb{Z}^\dagger\left[\frac{1_{BB}}{1_{BB}-G_{BB}(E)W_{BB}}\right]\mathbb{Z}\\
&= \frac{1}{(\mathbb{Z})^{-1}[1_{BB}-G_{BB}(E)W_{BB}](\mathbb{Z}^\dagger)^{-1}}\\
&= \frac{1}{1_{BB}-\mathbb{Z}^\dagger G_{BB}(E)W_{BB}\mathbb{Z}}\\
&= \frac{1}{1_{BB}-\mathbb{Z}^\dagger G_{BB}(E)\mathbb{Z}\mathbb{Z}^\dagger W_{BB}\mathbb{Z}}\\
&= \frac{1}{1_{BB}-\mathbb{F}\widetilde{\mathbb{G}}\widetilde{\mathbb{W}}} \qquad (26)
\end{aligned}$$

and noting that the Bloch state appearing in the ket of equation (10) can be written in the following form:

$$P_B\,[|E_o,\eta\rangle] = \begin{pmatrix} z_{1,\eta}\,\mathrm{e}^{\mathrm{i}\theta_\eta}\\ \vdots\\ z_{N,\eta}\,\mathrm{e}^{\mathrm{i}\theta_\eta}\\ \hline \vdots\\ \hline z_{1,\eta}\,\mathrm{e}^{\mathrm{i}(\mathcal{L}+1)\theta_\eta}\\ \vdots\\ z_{N,\eta}\,\mathrm{e}^{\mathrm{i}(\mathcal{L}+1)\theta_\eta}\end{pmatrix} = \mathbb{Z}\begin{pmatrix}(e_\eta)\,\mathrm{e}^{\mathrm{i}\theta_\eta}\\ \hline \vdots\\ \hline (e_\eta)\,\mathrm{e}^{\mathrm{i}(\mathcal{L}+1)\theta_\eta}\end{pmatrix}. \qquad (27)$$

3.6. Observation on the numerical precision and comparison with the Keldysh formalism

All the numerical data produced in this work has been obtained by means of Fortran codes implementing the Keldysh formalism (see [7]) or the Møller operator as presented in this paper. The two methods require different inputs. In particular, the Keldysh formalism requires the calculation of the Green's function of a semi-infinite perfect multichain. If one calculates this quantity by the method of decimation there might appear problems of numerical convergence, especially near to the points where the peaks described in this paper appear. This problem can be solved by controlling numerically the convergence of the decimation process, or by means of the following *analytic* expression:

$$G^{(\infty/2)} = \tfrac{1}{2}T^{-1}[(E-U)-(G^\infty)]T^{-1} \qquad (28)$$

where $G^{(\infty/2)}$ is the Green's function of a semi-infinite multichain projected on the left and on the right on the first column, and G^∞ is the Green's function of the corresponding infinite system projected on the left and on the right on the same column. This equation is valid under the hypothesis that the free hopping matrix T is Hermitian, i.e. $T = T^\dagger$ and invertible (I believe, however, that a generalization can be found). This equation can be demonstrated by taking an infinite multichain, dividing it into three separate regions (two semi-infinite multichains and a single column) and using standard linear algebra techniques to express the inverse of a matrix projected on a subspace as a function of the same matrix but projected on the complementary space (partition technique).

The numerical codes used in this work led to identical numerical results, also at the critical energies where the peaks appear. This proves that the numerical codes used are reliable and that the two formalisms are equivalent. Theoretically, however, there is a difference between the two formalisms: while the Keldysh formalism is 'local' in the sense that one has to perform a series of matrix multiplications from one side to the other of the disordered region, the Møller operator is 'global' in the sense that it requires to invert at once a matrix as big as the disordered region. This justifies intuitively the reason why the Møller operator is more adequate to describe the π-couplings since they arise from 'global' diagrams (in the sense that they go back and forth several times in the disordered region) as described in this paper.

4. Curves of constant average conductance: the '$w_G^2\mathcal{L}$ = *constant*' law

An important observation for the purposes of this paper is that, for any given kind of disorder (as specified by equation (3)), rescaling the global intensity of disorder w_G (as defined in equation (4)) and the length $\mathcal{L}$ such that $w_G^2\mathcal{L}$ = constant, produces systems having (almost) the same average conductance $\langle g(E)\rangle$. Figures 4(a) and (b) show a few representative examples illustrating this scaling law.

Consequently, if the average conductance is plotted versus the variables $(\mathcal{L}, 1/w_g^2)$, within a certain approximation the curves of constant height are rays passing through the origin. This scaling law is best obeyed in the limit $\mathcal{L}\to\infty$ (according to numerical simulation) and with no exceptions in energy (including the energies where the peaks arise). However, near to the peaks and around the energies where the free density of states (DOS) diverges, the convergence of $\langle g(E)\rangle_{w_G^2\mathcal{L}=\mathrm{const}}$ for $\mathcal{L}\to\infty$ is slower (see, e.g., figure 4(a) at $E = 1$).

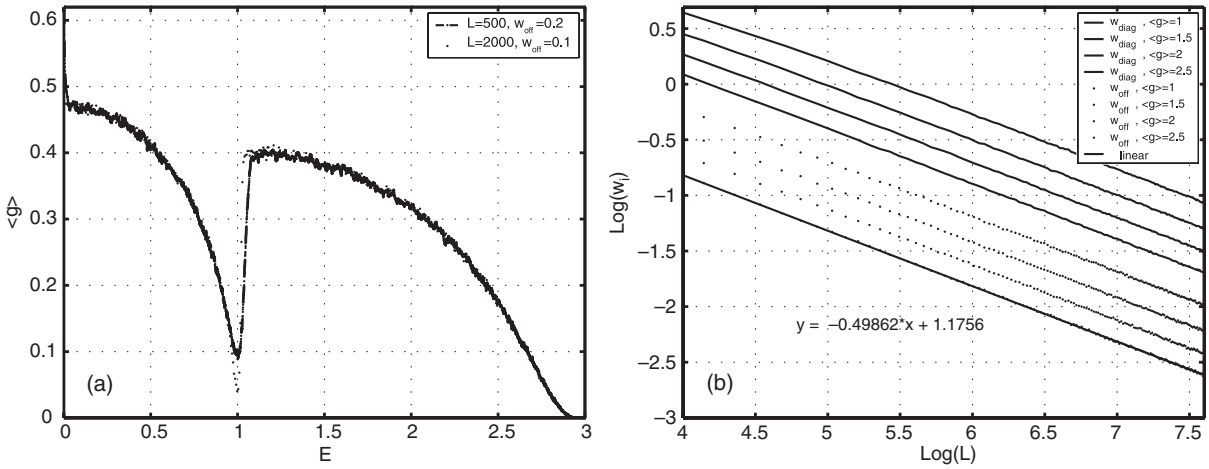

Figure 4. (a) Comparison of the average conductance of two rescaled systems: the first has $\mathcal{L} = 2000$, the second $\mathcal{L} = 500$, but they satisfy the condition $w_G^2\mathcal{L} =$ constant. (b) Typical plot of pairs of values $(w_G, \mathcal{L})$ for which the average conductance is constant (see the legend).

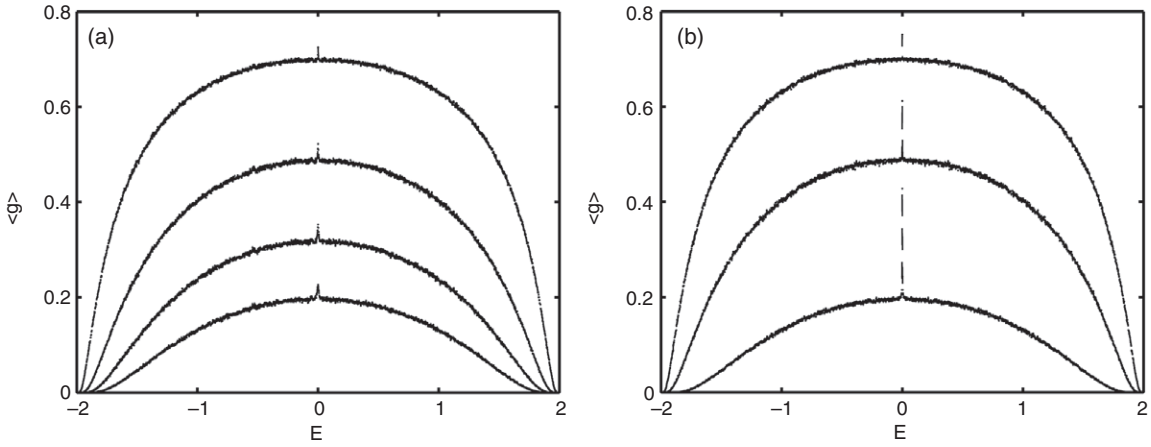

Figure 5. Average conductance for different amounts of diagonal disorder (a) and real off-diagonal disorder (b).

5. Results for one-dimensional systems ($N = 1$)

At first I consider truly one-dimensional systems ($N = 1$) with pure diagonal or real off-diagonal disorder. These types of disorders are often considered in the literature. One-dimensional systems always have a π-coupling at the center of the energy spectrum (see section 3.2).

5.1. Diagonal disorder

The curves in figure 5 represent a typical profile of the average conductance for a system with diagonal disorder, with the peaks at $E = 0$ clearly visible. According to equation (14), when the energy is varied, not only do the Bloch angles θ^+ and θ^- change, but so does the value of the Green's function $\widetilde{G}_{1,1}$. Hence, it is interesting to calculate numerically the average conductance in the (θ^+, θ^-) plane keeping $\widetilde{G}_{1,1}$ fixed. A typical result of such a simulation is presented in figure 6(a). This plot shows clearly that, when the difference $\theta^+ - \theta^-$ equals an integer multiple of π, the average conductance acquires an additional contribution over a *flat* background value. The features of figure 6(a) can be illustrated by performing the perturbative expansion of the Møller operator.

The strength of diagonal disorder will be abbreviated here as w_d (i.e. $w_d \equiv w^U_{1,1}$).

Developing the denominator of (10) as done in equation (25), and assuming for simplicity that $\widetilde{G}_{1,1} = -\mathrm{i}$, it can be shown that average conductance is given by

$$\begin{aligned}\langle g(E)\rangle &= \langle |A^{\mathrm{T}}_{1\to 1}|^2\rangle \\ &= \Bigg\langle \Bigg(f - \mathrm{i}w_d \sum_a \chi_a f_a - w_d^2 \sum_{ab} \chi_a\chi_b f_{ab} \\ &\quad + \mathrm{i}w_d^3 \sum_{abc} \chi_a\chi_b\chi_c f_{abc} + w_d^4 \sum_{abcd} \chi_a\chi_b\chi_c\chi_d f_{abcd} \Bigg) \\ &\quad \times \Bigg(\overline{f} + \mathrm{i}w_d \sum_a \chi_a \overline{f_a} - w_d^2 \sum_{ab} \chi_a\chi_b \overline{f_{ab}} \\ &\quad - \mathrm{i}w_d^3 \sum_{abc} \chi_a\chi_b\chi_c \overline{f_{abc}} + w_d^4 \sum_{abcd} \chi_a\chi_b\chi_c\chi_d \overline{f_{abcd}} \Bigg) \Bigg\rangle \\ &\quad + \mathrm{O}(w_d^6) \end{aligned} \tag{29}$$

where the $f_\cdot$ take into account the phase of the particular path followed.

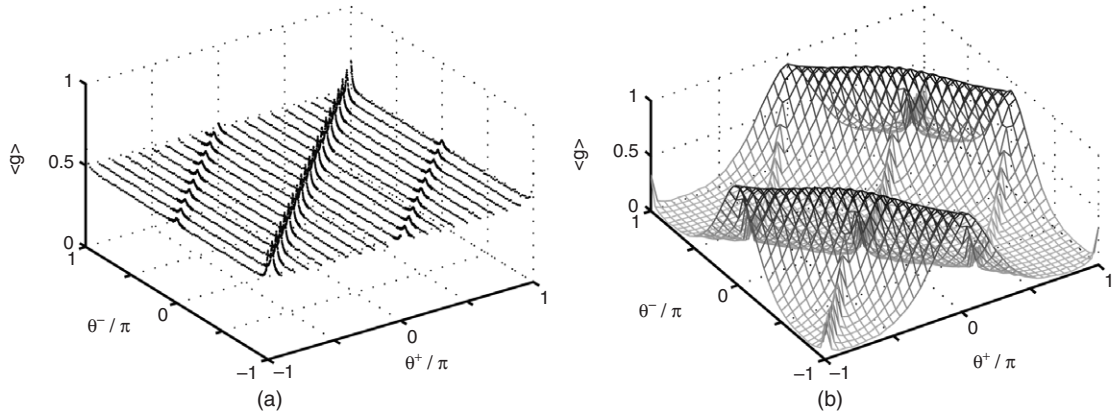

Figure 6. Average conductance as a function of θ^+ and θ^- for diagonal (a) and real off-diagonal (b) disorder. The other parameters appearing in equation (14) are held fixed. It is clearly visible that a resonance occurs when the difference $\theta^+ - \theta^-$ equals an integer multiple of π.

After some calculations, one arrives at the following result:

$$\langle g(E)\rangle = 1 - w_{\rm d}^2\mathcal{L}\langle\chi^2\rangle + w_{\rm d}^4\mathcal{L}^2(\langle\chi^2\rangle)^2 \times\left\{1 + \frac{2}{\mathcal{L}^2}\sum_{a<b}^{\mathcal{L}}\left[\cos\left[2(\theta^+ - \theta^-)(b-a)\right] + \cos\left[(\theta^+ - \theta^-)(b-a)\right]\right]\right\} + \mathrm{O}(w_{\rm d}^6). \quad (30)$$

Notice that the quantity $\frac{2}{\mathcal{L}^2}\sum_{a<b}^{\mathcal{L}}\cos[2(\theta^+ - \theta^-)(b-a)]$ goes to zero for $\mathcal{L}\to\infty$ unless $\theta^+ - \theta^-$ is an integer multiple of π. In the latter case the fourth-order term acquires an additional contribution, causing (together with higher orders) a peak in the conductance. Analogously, the term $\frac{2}{\mathcal{L}^2}\sum_{a<b}^{\mathcal{L}}\cos[(\theta^+ - \theta^-)(b-a)]$ goes to zero for $\mathcal{L}\to\infty$ unless $\theta^+ - \theta^-$ is an integer multiple of 2π, when the fourth-order term acquires again an additional contribution.

5.2. Real off-diagonal disorder

Similarly to the diagonal disorder case, the average conductance as a function of the energy shows peaks at $E = 0$ (see figure 5(b)).

Analogously, in the (θ^+, θ^-) plane the average conductance shows resonances whenever the difference $\theta^+ - \theta^-$ equals an integer multiple of π (see figure 6(b)).

Consider again the expansion of the average conductance (the strength of off-diagonal disorder is abbreviated to w_f and it is assumed again that $\widetilde{G}_{1,1} = -i$). In this case the following result is obtained:

$$\langle g(E)\rangle = 1 - w_f^2\mathcal{L}\langle\chi^2\rangle[2 + 2\cos(\theta^+ + \theta^-)] + \mathrm{O}(w_{\rm d}^4) \quad (31)$$

which very well describes the qualitative behavior in the (θ^+, θ^-) plane where there is no peak (figure 6(b)).

The peaks are caused by higher-order terms. The third order vanishes and the fourth order acquires the following additional contribution when the condition $\theta^+ - \theta^- = \pm\pi$ is satisfied:

$$\langle g(E)\rangle \to \langle g(E)\rangle + w_f^4\mathcal{L}^2(\langle\chi^2\rangle)^2\,\mathrm{Re}[(\mathrm{e}^{\mathrm{i}\theta^+} + \mathrm{e}^{\mathrm{i}\theta^-})^4] + \mathrm{O}(w_f^6). \quad (32)$$

In the case that $\theta^+ = -\theta^-$ (i.e. when the hoppings of the periodic system are real) and $\theta^+ = \pi/2$, $\mathrm{Re}[(\mathrm{e}^{\mathrm{i}\theta^+} + \mathrm{e}^{\mathrm{i}\theta^-})^4] = 16$, consistently with equation (37).

5.3. Definition of $\langle g\rangle_{\rm reg}$ and $\langle g\rangle_{\rm res}$

As illustrated in sections 5.1 and 5.2, it is possible to define, at every given order in the expansion, two different contributions to the average conductance, i.e. a regular part which is not sensitive to the validity of the resonant condition and a resonant part which is relevant only when the resonance sets in. One can more generally define:

- $\langle g\rangle_{\rm reg}$ = sum of all the diagrams whose contribution is *not* sensitive to the validity of the condition $\theta^+ - \theta^- = \pi$ in the limit $\mathcal{L}\to\infty$ with $w_{\rm G}^2\mathcal{L}$ = constant. These diagrams are called '*regular*'.
- $\langle g\rangle_{\rm res}$ = sum of all the diagrams whose contribution *is* sensitive to the validity of the condition $\theta^+ - \theta^- = \pi$ in the limit $\mathcal{L}\to\infty$ with $w_{\rm G}^2\mathcal{L}$ = constant. These diagrams are called '*resonant*'.
  In more formal terms, a diagram belongs to this class if and only if its ensemble-averaged value $d(\theta^+, \theta^-, \mathcal{L}, w_{\rm G})$ is such that

$$\lim_{\mathcal{L}\to\infty}\left[\lim_{(\theta^+-\theta^-)\to\pi} d\right] \neq \lim_{(\theta^+-\theta^-)\to\pi}\left[\lim_{\mathcal{L}\to\infty} d\right], \quad (33)$$

  with $w_{\rm G}^2\mathcal{L}$ = constant (it is also assumed that all the limits do exist). It turns out that a diagram belonging to this class gives always a negligible contribution if the resonant condition is not satisfied, i.e. $\lim_{(\theta^+-\theta^-)\to\pi}[\lim_{\mathcal{L}\to\infty} d] = 0$. The lowest-order diagrams belonging to this category are of the fourth order.

Since the definitions of $\langle g\rangle_{\rm reg}$ and $\langle g\rangle_{\rm res}$ are complementary, the total average conductance can be written as the sum of the regular and of the resonant contribution:

$$\langle g\rangle_{\rm tot} = \langle g\rangle_{\rm reg} + \langle g\rangle_{\rm res} \quad (34)$$

and, away from any π-coupling:

$$\langle g\rangle_{\rm tot} = \langle g\rangle_{\rm reg}. \quad (35)$$

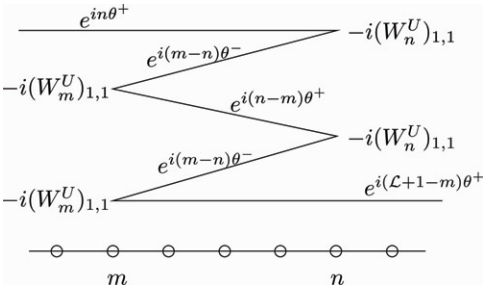

Figure 7. First diagram contributing to $\langle g\rangle_{\rm res}$ for $\theta^+ - \theta^- = \pi$. When the position of a scatterer is shifted by one unit, the diagram acquires an additional phase equal to $e^{i2(\theta^+-\theta^-)} = 1$, leading to a coherent sum over n and m.

From the latter equation it follows that the effects of the Anderson localization (as known when no anomaly sets in) are entirely contained in $\langle g\rangle_{\rm reg}$; the behaviors of $\langle g\rangle_{\rm reg}$ and $\langle g\rangle_{\rm res}$ are in principle two factorized problems, each with its own behavior.

Finally, the fourth-order diagram (lowest order) contributing to $\langle g\rangle_{\rm res}$ is depicted for diagonal disorder in figure 7. The examination of this diagram reveals what distinguishes the regular from the resonant diagrams: in a resonant diagram, when the position of a scatterer is shifted by one unit the diagram acquires an additional phase equal to $e^{i2n(\theta^+-\theta^-)} = 1$ with n integer, leading to a coherent sum.

5.4. Calculation of the perturbative expansion of $\langle g\rangle_{\rm res}$ up to the 12th order for $\theta^+ = -\theta^- = \pi/2$

By means of a numerical code, the expansion of $\langle g\rangle_{\rm res}$ was calculated up to the 12th order for both diagonal and real off-diagonal disorder. Terms of the form $w^{2n}\mathcal{L}^m$ with $m < n$ were neglected (see section 4).

For diagonal disorder and choosing $T_{1,1} = -\frac{1}{2}$ together with $\langle\chi^2\rangle = 1$, the following result is obtained:

$$\langle g(E=0)\rangle_{\rm res} = \frac{2}{2!}w_{\rm d}^4\mathcal{L}^2 - \frac{42}{3!}w_{\rm d}^6\mathcal{L}^3 + \frac{888}{4!}w_{\rm d}^8\mathcal{L}^4 - \frac{24\,336}{5!}w_{\rm d}^{10}\mathcal{L}^5 + \frac{1521\,631}{6!}w_{\rm d}^{12}\mathcal{L}^6 + \cdots. \quad (36)$$

For off-diagonal disorder, assuming further that $\theta^+ = \theta^- = \pi/2$ (i.e. not only $\theta^+ - \theta^- = \pi$), the result is

$$\langle g(E=0)\rangle_{\rm res} = \frac{32}{2!}w_f^4\mathcal{L}^2 - \frac{1664}{3!}w_f^6\mathcal{L}^3 + \frac{112\,640}{4!}w_f^8\mathcal{L}^4 - \frac{10\,698\,752}{5!}w_f^{10}\mathcal{L}^5 + \frac{1392\,902\,144}{6!}w_f^{12}\mathcal{L}^6 + \cdots. \quad (37)$$

It is not obvious whether these series are convergent in some sense. However, a comparison of these two series with numerical data shows that, at least for low disorder, higher orders lead to better fits (see section 5.5). Moreover the calculation of these expansions showed that, within any given order, different kinds of diagrams always contribute with the same sign for off-diagonal disorder, whereas they have different signs for diagonal disorder. This partially explains why the second series has much larger coefficients than the first one.

5.5. Comparison of the expansion of $\langle g\rangle_{res}$ with the numerical data

By calculating the difference of the average conductance at $E = 0$ and at a slightly different energy (in this case $E = 0.1$), it is possible to evaluate numerically the height of the peak and compare the curve obtained with the expansions (36) and (37). The results are shown respectively in figures 8(a) and (b).

6. Results for two coupled chains ($N = 2$)

Two coupled chains are the simplest systems which can have a π-coupling away from the center of the energy spectrum. Moreover, the π-coupling can occur between different combinations of bands. The fourth order in the expansion remains the lowest order contributing to the resonance and can be used to make important predictions.

6.1. Fourth order for two coupled chains and two resonating bands

This case is illustrated as an example at the energy $E = 0.3$ of figure 9. Taking care of all the angle combinations which form a π-coupling it can be seen that the fourth order of

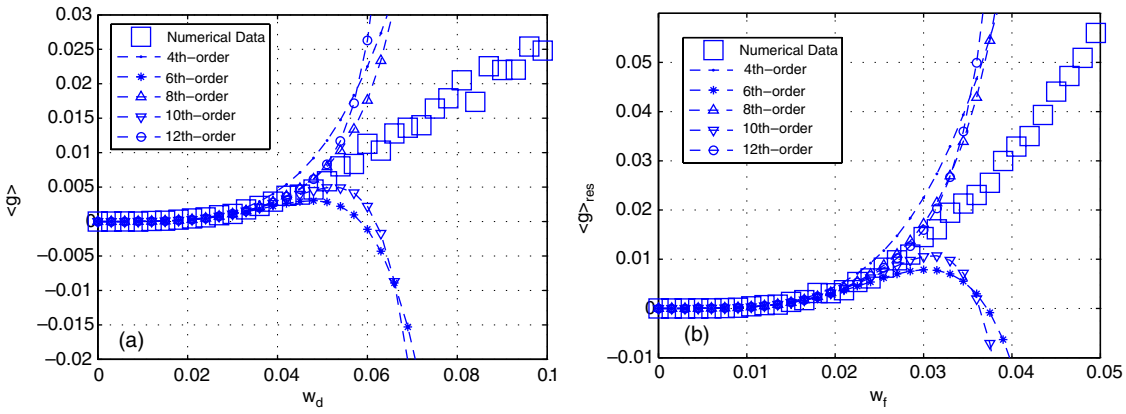

Figure 8. Comparison of the numerical data of $\langle g\rangle_{\rm res}$ for diagonal (a) and real off-diagonal (b) disorder with their expansion up to the 12th order. The length of the disordered region is in both cases $\mathcal{L} = 2000$.

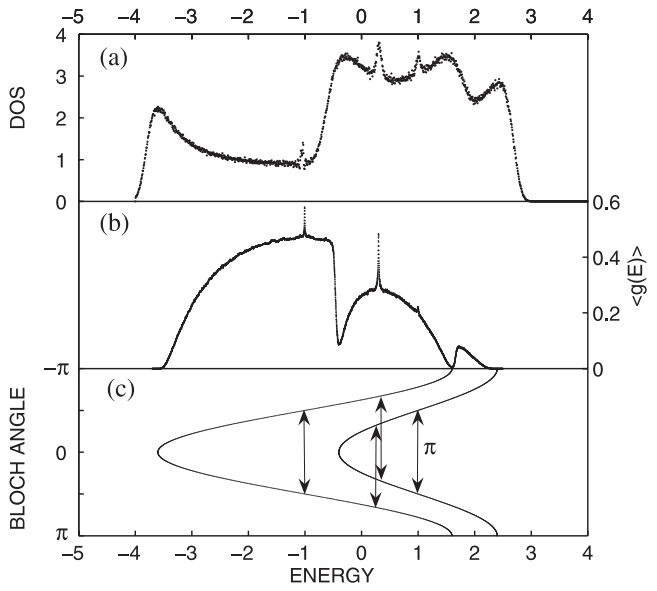

Figure 9. Average DOS in arbitrary units (a), average conductance (b) and band structure (c) of the two coupled chains defined by equation (46). The density of states corresponds to the disordered region (device) isolated from the leads. There are three energies at which a π-coupling occurs. At these energies, the average conductance and the density of states are peaked.

$\langle g\rangle_{\rm res}$ is given by the following equation (it is assumed that $\theta_2^+ - \theta_1^- = \pi$ and $\theta_1^+ - \theta_2^- = \pi$):

$$\begin{aligned}\langle g\rangle_{\rm res}^{(4)} = \frac{\mathcal{L}^2}{2!}\langle {\rm Tr}(&P_1M_mP_1M_nP_2M_mP_2M_nP_1\\ &+ P_1M_mP_2M_nP_1M_mP_2M_nP_1\\ &+ P_1M_mP_2M_nP_2M_mP_1M_nP_1\\ &+ P_2M_mP_2M_nP_1M_mP_1M_nP_2\\ &+ P_2M_mP_1M_nP_2M_mP_1M_nP_2\\ &+ P_2M_mP_1M_nP_1M_mP_2M_nP_2)\rangle + {\rm c.c.}\end{aligned} \tag{38}$$

where n and m are two different column indexes arbitrarily chosen and

$$M_n = \widetilde{G}\widetilde{W}_{U,n}Z + F^-\widetilde{G}\widetilde{W}_{T,n} + \widetilde{G}\widetilde{W}_{T,n}^\dagger F^+, \tag{39}$$

$$M_m = \widetilde{G}\widetilde{W}_{U,m} + \widetilde{G}\widetilde{W}_{T,m}F^- + F^+\widetilde{G}\widetilde{W}_{T,m}^\dagger, \tag{40}$$

where

$$P_1 = \begin{pmatrix}1&0\\0&0\end{pmatrix}, \qquad P_2 = \begin{pmatrix}0&0\\0&1\end{pmatrix}, \qquad F^\pm = \begin{pmatrix}{\rm e}^{\pm{\rm i}\theta_1^\pm}&0\\0&{\rm e}^{\pm{\rm i}\theta_2^\pm}\end{pmatrix}, \tag{41}$$

$$\widetilde{W}_{U(T),i} = Z^\dagger W_{U(T),i}Z, \qquad \widetilde{G} = Z^\dagger G Z. \tag{42}$$

In order to illustrate the origin of the terms in equation (38), consider as an example the first term, i.e. $P_1M_mP_1M_nP_2M_mP_2M_nP_1$. This product of matrices should be read from the right to the left. It represents an electron which arrives from the first band (projector P_1), scatters in n (M_n), propagates in the second band (P_2) up to the impurity on-site m and so on. Every term of equation (38) represents a different combination of the bands used to propagate, and corresponds to a generalization of the diagram seen in figure 7. Including the correct permutations of the bands involved, equation (38) can be generalized to any number of chains.

6.2. Fourth order for two coupled chains and only one resonating band

This case is illustrated as an example at the energies $E = 1$ of figure 9.

The fourth order of $\langle g\rangle_{\rm res}$ in the case that $\theta_1^+ - \theta_1^- = \pi$ and $\theta_2^+ - \theta_2^- \neq \pi$ is given by the following equation:

$$\langle g\rangle_{\rm res}^{(4)} = \frac{\mathcal{L}^2}{2!}\langle {\rm Tr}\left(P_1M_mP_1M_nP_1M_mP_1M_nP_1\right)\rangle + {\rm c.c.} \tag{43}$$

where the symbols have the same meaning as in equation (38).

In order to illustrate some properties of the previous expression, consider the example where $\theta_1^+ = -\theta_1^- = \frac{\pi}{2}$ and the matrices Z and G are given by

$$Z \equiv \frac{1}{\sqrt{2}}\begin{pmatrix}1&1\\1&-1\end{pmatrix}; \qquad \widetilde{G} = \begin{pmatrix}-\frac{\rm i}{2}&0\\0&\widetilde{G}_{2,2}\end{pmatrix}. \tag{44}$$

Using only off-diagonal disorder and assuming $w_{1,2}^T = w_{2,1}^T = 0$, the result is

$$\langle g\rangle_{\rm res}^{(4)} = \tfrac{1}{32}\,{\rm Re}\left(\langle (W_{1,1}^T)^2\rangle + \langle (W_{2,2}^T)^2\rangle - \langle (W_{1,2}^U)^2\rangle\right)^2\mathcal{L}^2. \tag{45}$$

The latter expression shows an interesting feature: the two kinds of off-diagonal disorder (on the T and on the U matrices) *compete* with each other.

6.3. Example of resonances without energy symmetry

The cases where π-coupling between the bands occurs for energies different from the center of the energy spectrum or only between a subgroup of all the bands are interesting because in these cases the (chiral or bipartite) sublattice symmetry claimed in references [15, 19] is broken. An example of this occurs for the system defined by

$$U = \begin{pmatrix}0&-1\\-1&0\end{pmatrix}; \qquad T = \begin{pmatrix}-1&-0.3\\-0.3&-1\end{pmatrix}. \tag{46}$$

The band structure of this system is shown in figure 9(c). It can be seen that there are three energies at which a π-coupling occurs. At the energy $E = -1$ and 1 only one band is involved, while at the energy $E = 0.3$ a π-coupling occurs between two bands. Notice that only the resonances occurring at $E = 0.3$ and 1 can be treated according to this formalism since *all* the bands must be present.

In figure 9(a) the density of states is shown and in figure 9(b) the average conductance for the two-chains system with off-diagonal disorder. The energy band structure of the perfect underlying system is presented in figure 9(c).

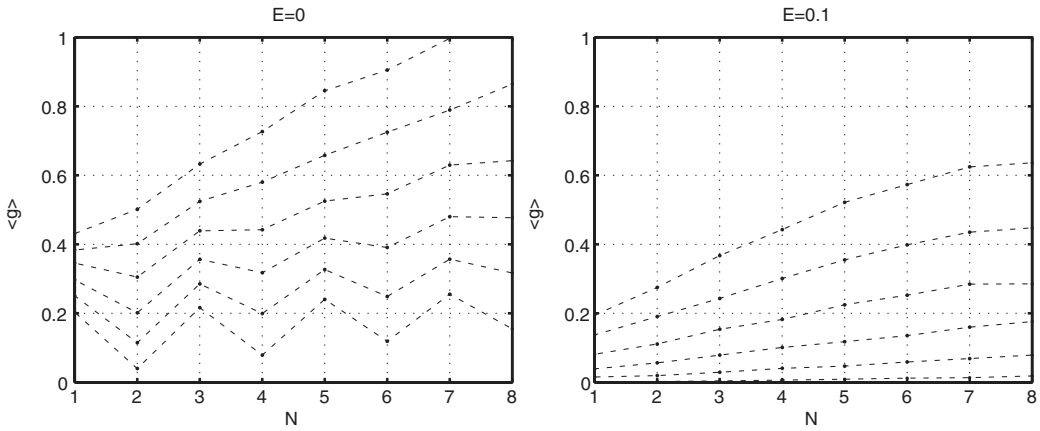

Figure 10. Average conductances as a function of the number N of chains. The left plot is calculated at $E = 0$ where the resonant contribution is not vanishing, while the right plot is calculated at $E = 0.1$. Different curves correspond to different amounts of *off-diagonal* disorder. The resonant contribution for odd numbers of chains is higher than for the even numbers.

6.4. Observation on the density of states

Detaching the disordered region (device) from the perfect leads and calculating numerically the spectrum of eigenvalues for many different disorder configurations, the average DOS of the disordered region alone was obtained. An example of this is depicted in figure 9(a). This figure is evidence for a direct connection between the peaks in the conductance and the peaks in the density of states. To the best of my knowledge, such a connection has previously been demonstrated only for strictly one-dimensional systems [24]. I performed numerous simulations for many different systems, and I always observed that, if a peak in the DOS is present, it occurs at the energies where there is a π-coupling. Therefore, this indicates that not only the conductance but also the DOS is intimately related to the band structure of the periodic system underlying the disorder.

7. Even–odd effect

Several studies have reported that coupled quantum chains might show even–odd effects [3, 2, 4, 18, 19, 26]. Here it is shown that π-coupling can induce an even–odd effect on the average conductance. To the best of my knowledge, this effect has been observed for the first time by monitoring the localization length in similar systems, see [4]. Taking a family of systems with T given by minus the identity and U having -1 around the diagonal and zero elsewhere, I could see that the resonant contribution $\langle g\rangle_{\rm res}$ has oscillations as a function of the number of chains while the regular part $\langle g\rangle_{\rm reg}$ does not show this feature. This result leads to oscillations in the conductance for $E = 0$ shown in figure 10 (for any given number of chains these systems have π-couplings at $E = 0$). I have performed simulations with both diagonal and off-diagonal disorder, but only the latter case shows this feature.

8. Conclusion

The message of this paper is that the band structure of the perfect system underlying the disorder contains essential information for the anomalies in the conductance and in the density of states. I have proved that the peaks in the conductance are caused by the resonant contribution $\langle g\rangle_{\rm res}$ defined in this paper, and that no further symmetry hypothesis is needed to explain these anomalies. I have also shown that the resonant contribution is responsible for an even–odd effect of the average conductance. The formalism presented in this paper is a very powerful tool for understanding delocalization in disordered multichain systems, and makes it possible to construct analytical expressions to tune the parameters of the system so as to obtain high conductance peaks in the chosen spectral regions.

Acknowledgments

I wish to thank G Grosso for the many useful discussions and A Cresti for having provided me with a numerical code based on the Keldysh formalism [7] used as a check and for faster simulations.

References

[1] Apalkov V M, Raikh M E and Shapiro B 2004 Anomalously localized states in the Anderson model *Phys. Rev. Lett.* **92** 066601
[2] Brouwer P W, Mudry C and Furusaki A 2000 Density of states in coupled chains with off-diagonal disorder *Phys. Rev. Lett.* **84** 2913–6
[3] Brouwer P W, Mudry C, Simons B D and Altland A 1998 Delocalization in coupled one-dimensional chains *Phys. Rev. Lett.* **81** 862–5
[4] Chan W L, Wang X R and Xie X C 1996 Differences between random-potential and random-magnetic-field localization in quasi-one-dimensional systems *Phys. Rev.* B **54** 11213–8
[5] Cheraghchi H 2006 Scaling properties of one-dimensional off-diagonal disorder *J. Stat. Mech.* P11006
[6] Chiappe G, Louis E, Sanchez M J and Verges J A 2004 Classical trajectories in quantum transport at the band center of bipartite lattices with or without vacancies *Phys. Rev.* B **69** 201405
[7] Cresti A, Farchioni R, Grosso G and Parravicini G P 2003 Keldysh–Green function formalism for current profiles in mesoscopic systems *Phys. Rev.* B **68** 075306

[8] Deych L I, Erementchouk M V, Lisyansky A A and Altshuler B L 2003 Scaling and the center-of-band anomaly in a one-dimensional Anderson model with diagonal disorder *Phys. Rev. Lett.* **91** 096601
[9] Eggarter T P and Riedinger R 1978 Singular behavior of tight-binding chains with off-diagonal disorder *Phys. Rev.* B **18** 569–75
[10] Garcia-Garcia A M and Cuevas E 2006 Anderson transition in systems with chiral symmetry *Phys. Rev.* B **74** 113101
[11] Goldberger M L and Watson K M 1964 *Collision Theory* (New York: Wiley)
[12] Goldhirsch I, Noskowicz S H and Schuss Z 1994 Spectral degeneracy in the one-dimensional Anderson problem—a uniform expansion in the energy-band *Phys. Rev.* B **49** 14504–22
[13] Gor'kov L P and Dorokhov O N 1976 Singularities in the density of electronic states of one-dimensional conductors with disorder *Solid State Commun.* **20** 789–92
[14] Heinrichs J 2004 Anomalous scaling of conductance cumulants in one-dimensional Anderson localization *J. Phys.: Condens. Matter* **16** 7995–8005
[15] Inui M, Trugman S A and Abrahams E 1994 Unusual properties of midband states in systems with off-diagonal disorder *Phys. Rev.* B **49** 3190–6
[16] Kappus M and Wegner F 1981 Anomaly in the band center of the one-dimensional Anderson model *Z. Phys.* B **45** 15–21
[17] Motrunich O, Damle K and Huse D A 2002 Particle–hole symmetric localization in two dimensions *Phys. Rev.* B **65** 064206
[18] Mudry C, Brouwer P W and Furusaki A 1999 Random magnetic flux problem in a quantum wire *Phys. Rev.* B **59** 13221–34
[19] Mudry C, Brouwer P W and Furusaki A 2000 Crossover from the chiral to the standard universality classes in the conductance of a quantum wire with random hopping only *Phys. Rev.* B **62** 8249–68
[20] Mudry C, Ryu S and Furusaki A 2003 Density of states for the pi-flux state with bipartite real random hopping only: a weak disorder approach *Phys. Rev.* B **67** 064202
[21] Schomerus H and Titov M 2003 Band-center anomaly of the conductance distribution in one-dimensional Anderson localization *Phys. Rev.* B **67** 100201
[22] Soukoulis C M and Economou E N 1981 Off-diagonal disorder in one-dimensional systems *Phys. Rev.* B **24** 5698–702
[23] Theodorou G and Cohen M H 1976 Extended states in a one-dimensional system with off-diagonal disorder *Phys. Rev.* B **13** 4597–601
[24] Thouless D J 1972 Relation between density of states and range of localization for one-dimensional random systems *J. Phys. C: Solid State Phys.* **5** 77
[25] Titov M and Schomerus H 2005 Nonuniversality of Anderson localization in short-range correlated disorder *Phys. Rev. Lett.* **95** 126602
[26] Verges J A 2002 Conductance scaling at the band center of wide wires with pure nondiagonal disorder *Phys. Rev.* B **65** 054201
[27] Zhang Y Y and Xiong S J 2005 Statistics of Lyapunov exponents of quasi-one-dimensional disordered systems *Phys. Rev.* B **72** 132202
[28] Ziman T A L 1982 Localization with off-diagonal disorder—a qualitative theory *Phys. Rev.* B **26** 7066–9